Bull. Mater. Sci., Vol. 32, No. 2, April 2009, pp. 205–214. © Indian Academy of Sciences.

Spectroscopic, thermal and biological studies of coordination compounds of sulfasalazine drug: Mn(II), Hg(II), Cr(III), ZrO(II), VO(II) and Y(III) transition metal complexes

M G ABD EL-WAHED[†], M S REFAT* and S M EL-MEGHARBEL[†]

Department of Chemistry, Faculty of Science, Port Said, Suez Canal University, Port Said, Egypt
[†]Department of Chemistry, Faculty of Science, Zagazig University, Zagazig, Egypt

MS received 22 July 2008

Abstract. **The complexations of sulfasalazine (H_3Suz) with some of transition metals have been investigated. Three types of complexes, $[Mn(HSuz)^{-2}(H_2O)_4]\cdot 2H_2O$, $[M(HSuz)^{-2}(H_2O)_2]\cdot xH_2O$ (M = Hg(II), ZrO(II) and VO(II), $x = 4$, 8 and 6, respectively) and $[M(HSuz)^{-2}(Cl)(H_2O)_3]\cdot xH_2O$ (M = Cr(III) and Y(III), $x = 5$ and 6, respectively) were obtained and characterized by physicochemical and spectroscopic methods. The IR spectra of the complexes suggest that the sulfasalazine behaves as a monoanionic bidentate ligand. The thermal decomposition of the complexes as well as thermodynamic parameters (ΔE^*, ΔH^*, ΔS^* and ΔG^*) were estimated using Coats–Redfern and Horowitz–Metzger equations. *In vitro* antimicrobial activities of the H_3Suz and the complexes were tested.**

Keywords. **Infrared spectra; electronic spectra; thermal analysis; sulfasalazine; antimicrobial activity.**

1. Introduction

Sulfasalazine (figure 1, H_3Suz) is a sulfa drug, a derivative of Mesalazine (5-aminosalicylic acid abbreviated as 5-ASA), used primarily as an anti-inflammatory agent in the treatment of inflammatory bowel disease as well as for rheumatoid arthritis (Bell and Habal 1997; Diav-Citrin *et al* 1998; Sutherland *et al* 2000; Hanauer *et al* 2005).

When dealing with the interaction between drugs and metal ions in living systems, a particular interest has been given to the interaction of metal ions with antibiotics. Antibiotics that interact with metal ions constitute a class of drugs which has been widely used in medicine both towards human beings and animals (Klostersky *et al* 1973; Zaki *et al* 1974). In particular, the interaction between transition metals and β-lactamic antibiotics such as cephalexin has been recently investigated by several physicochemical and spectroscopic methods, and with detailed biological data (Abdel-Gawad *et al* 1987; Lozano and Borras 1987; Helaleh and Nameh 1998; Anacona 2001). Many drugs possess modified pharmacological and toxicological properties when administered in the form of metallic complexes. Probably the most widely studied cation in this respect is Cu(II), since a host of low-molecular-weight copper complexes have been proven beneficial against several diseases such as tuberculosis, rheumatoid, gastric ulcers, and cancers (Williams 1971; Sorenson 1976; Brown *et al* 1980; Ruiz *et al* 1995).

In the literature survey, there is little attention concerning the mode of coordination of sulfasalazine with metal ions. Previous studies (Mukherjee *et al* 1993; Tabassum *et al* 1996; Chen *et al* 2003, 2008; Kang *et al* 2006; Yuan *et al* 2006; Golzar Hossain 2007) of the complexation of sulfa drugs did not focus on the coordination behaviour, but only dealt with the solution state and crystal structures of its metal complexes.

In our previous work, with respect to metal drug complexes, the synthesis, structural, thermal and biological studies of folic acid, allopurinol, amiloroide HCl and chloramphenicol complexes with *d*-block metal ions have been discussed (Refat 2007; Abd El-Wahed *et al* 2008a–d). For continuity, we have employed in this study the coordination mode of sulfasalazine (H_3Suz) complexes via some of *d*-block such as Mn(II), Hg(II), Cr(III), ZrO(II), VO(II) and Y(III). The solid products were isolated and characterized by elemental analysis CHN, molar conductance, magnetic moment and thermal analyses.

2. Experimental

2.1 *Physical measurements*

Carbon and hydrogen contents were determined using a Perkin-Elmer CHN 2400. The metal content was found gravimetrically by converting the complexes into their corresponding oxides.

*Author for correspondence (msrefat@yahoo.com)

Table 1. Elemental analyses and physical data of sulfasalazine and its complexes.

Complexes	*M* (wt.)	mp (°C)	Colour	Magnetic moment	Content ((calculated) found) % C	% H	% N	% Cl	% M	Λm (Ω^{-1} cm^{-1} mol^{-1})
$[Mn(SuzH)(H_2O)_4]2H_2O$ ($C_{18}H_{24}N_4O_{11}S$ Mn)	558·93	>300	Black	1·90	(38·64) 38·14	(4·29) 4·30	(10·01) 9·97	–	(9·82) 9·75	22
$[Hg(SuzH)(H_2O)_2]4H_2O$ ($C_{18}H_{24}N_4O_{11}S$ Hg)	705	>300	Buff		(30·63) 30·61	(3·40) 3·39	(7·94) 7·96	–	(28·51) 28·12	24
$[Cr(SuzH)(Cl)(H_2O)_3]5H_2O$ ($C_{18}H_{28}N_4O_{13}S$ Cl Cr)	627·50	250	Dark brown	2·00	(34·42) 34·32	(4·46) 4·38	(8·92) 8·86	(5·65) 5·64	(8·28) 8·24	96
$[ZrO(SuzH)(H_2O)_2]8H_2O$ ($C_{18}H_{32}N_4O_{15}S$ ZrO)	683·2	>300	Orange		(31·61) 31·40	(4·68) 4·70	(8·19) 8·22	–	(15·69) 15·52	23
$[VO(SuzH)(H_2O)_2]6H_2O$ ($C_{18}H_{28}N_4O_{13}S$ VO)	606·94	>300	Dark brown		(35·58) 35·54	(4·61) 4·59	(9·22) 9·19	–	(11·02) 10·98	25
$[Y(SuzH)(Cl)(H_2O)_3]6H_2O$ ($C_{18}H_{30}N_4O_{14}S$ Cl Y)	682·40	>300	Orange		(31·65) 31·18	(4·39) 4·58	(8·20) 8·68	(5·20) 5·48	(13·02) 13·16	88

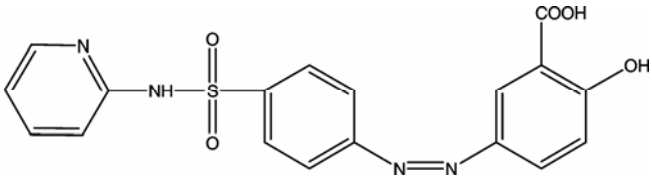

Figure 1. Sulfasalazine (H_3Suz).

Infrared spectra were recorded on Bruker FTIR Spectrophotometer (4000–400 cm^{-1}) in KBr pellets. The UV–Vis spectra were studied in the DMSO solvent with a concentration of $1·0 \times 10^{-3}$ M for the H_3Suz and their complexes using Jenway 6405 Spectrophotometer with 1cm quartz cell, in the range 800–200 nm. Molar conductances of the freshly prepared solutions of the H_3Suz complexes with $1·0 \times 10^{-3}$ M in DMSO were measured using Jenway 4010 conductivity meter. Magnetic measurements were carried out on a Sherwood Scientific magnetic balance using Gouy method. ^{1}H-NMR spectra were recorded on a Varian Gemini 200 MHz spectrometer using DMSO-d_6 as solvent. Thermogravimetric analyses (TGA and DTG) were carried out in a dynamic nitrogen atmosphere (30 ml/min) with a heating rate of 10 C/min using a Shimadzu TGA-50H thermal analyser.

2.2 *Antimicrobial activity test*

According to Gupta *et al* (1995), the hole well method was applied. The investigated isolates of bacteria were seeded in tubes with nutrient broth (NB). The seeded NB (1 cm^3) was homogenized in the tubes with 9 cm^3 of melted (45°C) nutrient agar (NA). The homogeneous suspensions were poured into Petri dishes. The holes (diameter, 4 mm) were done in the cool medium. After cooling, 2×10^{-3} dm^3 of the investigated compounds were applied using a micropipette. After incubation for 24 h in a thermostat at 25–27°C, the inhibition (sterile) zone diameters (including disc) were measured and expressed in mm. An inhibition zone diameter of over 7 mm indicates that the tested compound is active against the bacteria under investigation.

The antibacterial activities of the investigated compounds were tested against *Escherichia coli* (Gram, –ve), *Bacillus subtilis* (Gram, +ve) and antifungal (tricoderma and penicillium activities).

2.3 *Materials and methods*

All chemicals used were of analytical grade where possible and were purchased from Aldrich and Merck companies and sulfasalazine drug was presented from Egyptian international pharmaceutical industrial company (EIPICo.). The complexes were prepared by mixing sulfasalazine (2 mmol) and metal chlorides: $MnCl_2·4H_2O$, $HgCl_2$, $CrCl_3$, $ZrOCl_2·xH_2O$, metal(II) sulfate: $VOSO_4·xH_2O$ and metal(III) nitrate: $Y(NO_3)_3·6H_2O$ (1 mmol) in mixed solvent MeOH/H_2O (50/50%; 40 cm^3), then pH of the solution was adjusted to 8–9 with 1 M NaOH solution and the reaction mixture was stirred at 60°C for 2 h and left to stand overnight. The precipitated complexes were filtered off, washed with MeOH and H_2O and dried *in vacuo* at room temperature under anhydrous $CaCl_2$.

3. Results and discussion

The elemental analysis (CHN) agrees quite well with the speculated structure of the coloured sulfasalazine complexes (table 1). Manganese(II) complex is black in colour, mercury(II) complex is buff, the chromium(III) and vanadyl(II) complexes are dark brown, while the zirconyl(II) and yttrium(III) complexes are orange in colour. They are thermally stable above > 250°C, soluble in DMSO and DMF. The conductivity values measured in DMSO at room

Table 2. Main IR data of sulfasalazine and its complexes.

Compound	ν(O–H)	ν(C–O)	δ(OH)	ν_{as}(COO)	ν_s(COO)	$\Delta\nu$(COO)	ν(M–O)
Mn(II)	3385	1253	1357	1598	1309	289	516 454
Hg(II)	3422	1231	1350	1594	1327	267	512 486
Cr(III)	3422	1233	1358	1598	1313	285	524 434
ZrO(II)	3419	1241	1355	1595	1318	277	525 492
VO(II)	3357	1260	1357	1588	1310	278	452 422
Y(III)	3350	1263	1360	1594	1313	281	524 439

temperature are located in the range of non-electrolytes (Geary 1971) for Mn(II), Hg(II), ZrO(II), and VO(II)/HSuz complexes while the chromium(III) and yttrium(III) complexes behave as 1 : 1 electrolytes. The interpretation concerning decreasing of conductivity values back to the deprotonation of both OH of carboxylic and OH of phenolic groups for the sulfasalazine ligand. This assumption proves that free ligand acts in a bidentate fashion via carboxylic and phenolic groups and also attributed to the participation of carboxylic group as a monodentate chelate.

Magnetic moments were performed according to the Gauy method (Lever 1980) and the value for the manganese(II) complex is 1·90 BM indicating that it has one unpaired electron. The chromium(III) complex has a magnetic moment equal to 2·00 BM as predicted by a low spin system with two unpaired electrons, hence, the Mn(II) and Cr(III) complexes formed have an octahedral configuration with d^2sp^3 hybrid orbital.

3.1 *Infrared spectra*

The infrared spectra of sulfasalazine and its complexes exhibited with the main coordination bands which reveals the mode of bonding and are summarized in table 2. Concerning the sulfasalazine complex, the most important region in the infrared spectra of all complexes and the H_3Suz free ligand ($\sim$1700–1300 cm^{-1}) is selected and assigned in table 2 as follows:

In contrast to the assignments data of Nor, Mn(II), Hg(II), Cr(III), ZrO(II), VO(II) and Y(III) complexes show no absorption band at 1677 cm^{-1}, characteristic of the ν(C=O) vibration of the carboxylic group (in case of free H_3Suz ligand), that is indicative of the involvement of the carboxylic group in the coordination with metal ion. The peaks at 1598 cm^{-1} (*vs*) for Mn(II)/HSuz, 1594 cm^{-1} (*s*) for Hg(II)/HSuz, 1598 cm^{-1} (*vs*) for Cr(III), 1595 cm^{-1} (*vs*) for ZrO(II)/HSuz, 1588 cm^{-1} (*s*) for VO(II)/HSuz and 1594 cm^{-1} (*s*) for Y(III)/HSuz complexes, respectively are absent in the spectrum data of the free H_3Suz and can be assigned to the asymmetric stretching vibration of the carboxylate group, $\nu_{as}(COO^-)$. The spectra of $[Mn(HSuz)^{-2}(H_2O)_4]\cdot 2H_2O$, $[M(HSuz)^{-2}(H_2O)_2]\cdot xH_2O$ (M = Hg(II), ZrO(II) and VO(II), x = 4, 8 and 6, respectively) and $[M(HSuz)^{-2}(Cl)(H_2O)_3]\cdot xH_2O$ (M = Cr(III) and Y(III), x = 5 and 6, respectively) complexes also have medium to strong intensity band in the range of 1309–1327 cm^{-1}. This band is absent in spectrum of Suz and interpretive to the symmetric vibration of the $\nu_s(COO^-)$ group.

Deacon and Phillips (1980) studied the criteria that can be used to distinguish between the three binding states of the carboxylate complexes. These criteria are: (i) $\Delta\nu >$ 200 cm^{-1} (where $\Delta\nu = [\nu_{as}(COO^-) - \nu_s(COO^-)]$), this relation is found in case of unidentate carboxylato complexes, (ii) bidentate or chelating carboxylato complexes exhibit $\Delta\nu$ significantly smaller than ionic values ($\Delta\nu <$ 100 cm^{-1}), and finally (iii) bridging complexes show $\Delta\nu$ comparable to ionic values ($\Delta\nu \sim$ 150 cm^{-1}). The observed $\Delta\nu$ for all the sulfasalazine complexes is >200 cm^{-1} which confirms a unidentate interaction of the carboxylate group.

A broad diffuse band of strong to medium strong intensity in the 3500–3350 cm^{-1} region may be assigned to the OH stretching vibration for the coordinated and uncoordinated water molecules in the H_3Suz complexes. It is noteworthy to say that when the media of precipitation is sodium hydroxide, this means that the sodium salt of sulfasalazine is formed, so, the stretching vibration band of ν(OH) of carboxylic group. As is also difficult distinction between the ν(OH) of phenolic group of sulfasalazine and the stretching vibrational bands of water molecules because of the overlapping values, and appear in one place.

To ascertain the involvement of ν(OH) of phenolic group of sulfasalazine in the coordination process to be followed by the stretching vibration bands of ν(C–O) in all sulfasalazine complexes, examination of the H_3Suz complexes found that the ν(C–O) shifted to lower wave number from 1278 cm^{-1} in case of free ligand to 1230 to

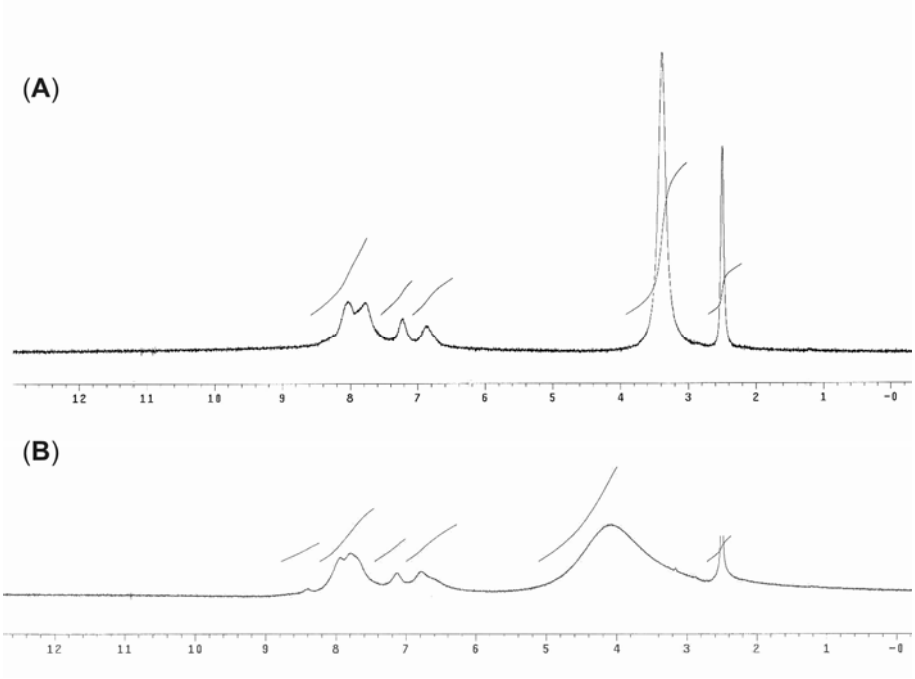

Figure 2. ^{1}H-NMR spectra of: (**A**) VO(II)/HSuz and (**B**) Y(III)/HSuz complexes.

1260 cm^{-1} in case of their complexes. This result indicates that the phenolic group participated in the complexation and the H_3Suz ligand acted as bidentate. The lower shift of δ(OH) from 1393 cm^{-1} in the free H_3Suz ligand to 1360–1350 cm^{-1} in their complexes is another factor confirming the involvement of OH phenolic group in the coordination process.

The presence of M–O stretching vibrations at two bands: 516 and 454 cm^{-1} for Mn(II)/HSuz, 512 and 486 cm^{-1} for Hg(II)/HSuz, 524 and 435 cm^{-1} for Cr(III)/HSuz, 525 and 492 cm^{-1} for ZrO(II)/HSuz, 452 and 422 cm^{-1} for VO(II)/HSuz and (524 and 439) for Y(III)/HSuz, respectively supports coordination by H_3Suz ligand as a bidentate monoanionic chelating agent via OH of carboxylic and phenolic groups (Nakamoto 1986).

3.2 *UV-Vis spectra*

The UV-Vis spectra of sulfasalazine and their complexes in DMSO exhibit and detect peaks which are tabulated in table 3. There are two absorption maxima peaks at ranges from 215–340 nm and 350–500 nm, assigned to π–π* and n–π* transitions within the organic moiety of sulfasalazine ligand. The electronic absorption spectra of all H_3Suz complexes show a bathchromic shift rather than free ligand within n–π* transition region. This shift is attributed to the place of complexation and the change in the electronic configuration for the H_3Suz complexes formed. The electronic spectrum with respect to the Mn(II)/HSuz complex shows a weak absorption peak in the visible region probably due to spin-orbit forbidden transitions.

3.3 *^{1}H-NMR spectra*

The ^{1}H-NMR spectra presented the persuasive confirmation of the coordination modes. Thus, the ^{1}H-NMR spectra of both VO(II)/HSuz and Y(III)/HSuz complexes (figures 2A and B) on comparing with those of spectrum of the free sulfasalazine indicate that, H_3Suz ligand acts as bidentate ligand through the phenolic OH group and carboxylic OH group. ^{1}HNMR spectra of vanadyl(II) and yttrium(III) complexes were carried out in DMSO-d_6 as a solvent, the data obtained are in agreement with the suggested coordination through the carboxylic and phenolic groups by absence of the signals of two protons which exist in the free ligand at about δ = 11·00 and 5·00 ppm, respectively and due to different chemical environments the signals of aromatic protons at 6·00–8·00 ppm are present with decreasing intensities.

3.4 *Thermal analysis and kinetic studies*

It seemed of interest to evaluate the effect of heating on the thermal stability of the prepared complexes in the same way as reported earlier (Refat 2007; Abd El-Wahed *et al* 2008a–d).

The results showed that the complexes lost its hydration water below 573 K. Within the temperature range 573–653 K the coordinated water molecules were liberated. The anhydrous complexes displayed the decomposition of the organic ligand within the temperature range 673–1073 K leading to metal oxide. The metal contents were calculated from the residual contents and were

found to be in good agreement with the results of elemental analysis. The sulfasalazine ligand melts at 552 K with simultaneous decomposition (figure 3). The thermal decomposition of (H_3SuZ) occurs completely in two steps which were observed at 552 and 1025 K corresponding to loss of $C_4H_6N_4SO_3$ and $C_2H_8O_2$ (organic moiety) representing a weight loss (obs = 47·20%, calc = 47·69) and (obs = 16·50%, calc = 16·00), respectively, then leaving residual carbon as final fragment.

[Mn(SuzH)$(H_2O)_4$]2H_2O complex was thermally decomposed in four successive decomposition steps within the temperature range 313–1073 K. The first decomposition step (obs = 6·69%, calc = 6·44) within the temperature range 313–403 K, may be attributed to the liberation of the two hydrated water molecules. The second and third decomposition steps found within the temperature range 423–703 K (obs = 12·43%, calc = 12·88), (obs = 13·82%, calc = 13·77), which are reasonably accounted for by the removal of 4H_2O and $C_2H_7NO_2$ (organic moiety), respectively. The rest of sulfasalazine molecule was removed on the fourth step within the temperature range 713–1073 K (obs = 39·60%, calc = 39·18). The decomposition of the ligand molecule ended with a final oxide residue of MnO and contaminated with residual carbon (27·23%, mass = 154·93).

The TG curve of [Hg(SuzH)$(H_2O)_2$]4H_2O complex indicates that the mass change begins at 367 K and continues up to 1053 K. The first mass loss corresponds to the liberation of the four hydrated water molecules (obs = 10·80%, calc = 10·21). The second decomposition step occurs in the range 463–653 K and corresponds to the loss of 2H_2O + $C_6H_8N_2SO_2$ (organic moiety) (obs = 29·12%, calc = 29·50). The final decomposition step occurs in the range 673–1073 K and corresponds to the loss of $C_4H_4N_2O_2$ (organic moiety) (obs = 29·12%, calc = 29·50). DTG profile shows three endothermic peaks. The first at 367 K corresponds to the melting of the complex, while the second at 527 K corresponds to the dehydration and decomposition of the complex. The third broad endothermic peak corresponds to the final decomposition of the organic ligand to the HgO + residual carbon atoms.

[Cr(SuzH)(Cl)$(H_2O)_3$]5H_2O was thermally decomposed in five successive decomposition steps within the temperature range 323–1073 K. The first decomposition step (obs = 7·39%, calc = 7·17) within the temperature range, 323–423 K, may be attributed to the liberation of two and half hydrated water molecules. The second and third decomposition steps found within the temperature range 443–813 K (obs = 15·69%, calc = 15·77), (obs = 6·45%, calc = 6·85), are reasonably accounted for by the removal of 5·5H_2O and C_2H_5N (organic moiety), respectively. The rest of sulfasalazine molecule was removed on the fourth and fifth steps within the temperature range 833–1073 K and corresponds to the loss of C_2H_4N and $C_5H_3N_2SO_{3.5}Cl$ (organic moiety) (obs = 6·56%, calc = 6·69), (obs = 33·86%, calc = 34·18), respectively. The decomposition of the ligand molecule ended with a final oxide residue of $CrO_{1.5}$ + contaminated carbon atoms.

[ZrO(SuzH)$(H_2O)_2$]8H_2O complex is thermally stable up to 323 K and decomposition beyond this temperature is indicated by the first loss step in the TG curve. The mass loss at 323 K corresponds to the loss of 2H_2O (obs = 5·67%, calc = 5·26). Continuous mass loss in the TG curve beyond 333 K, 373 K, 433 K and 616 K, corresponds to the loss of 8H_2O + NO. The rest of sulfasalazine molecule was removed on the six and seven steps within the temperature range 723–1073 K corresponding to the loss of N_2 + 3H_2 and 0·5N_2 + 3H_2 (obs = 4·39%, calc = 4·97), (obs = 2·29%, calc = 2·92), respectively. The DTG profile shows four endothermic peaks. The first and second peaks at 318, 373 K corresponds to the dehydration of the complex, while the third and fourth at 755, 1028 K corresponds to the final decomposition of the organic ligand to the $ZrOSO_4$ + carbon atoms residue.

Table 3. Electronic spectral data of the free sulfasalazine ligand and its complexes.

Compound	λ_{max} (nm)	ε (mol^{-1} cm^{-1})	Assignment
Sulfasalazine	225	790	π–π^* trans.
	280	3000	n–π^* trans.
	290	1892	n–π^* trans.
	360	2574	n–π^* trans.
	390	1188	n–π^* trans.
	415	1678	n–π^* trans.
Mn	225	3000	π–π^* trans.
	290	2405	n–π^* trans.
	360	2448	n–π^* trans.
	385	2254	n–π^* trans.
	440	2540	n–π^* trans.
	480	2828	n–π^* trans.
Hg	215	3000	π–π^* trans.
	240	946	π–π^* trans.
	290	1786	n–π^* trans.
	360	1330	n–π^* trans.
	390	1123	n–π^* trans.
	425	1771	n–π^* trans.
Cr	220	1389	π–π^* trans.
	295	1749	n–π^* trans.
	390	1153	n–π^* trans.
	440	1576	n–π^* trans.
ZrO	220	3000	π–π^* trans.
	295	3000	n–π^* trans.
	340	1807	n–π^* trans.
	390	1301	n–π^* trans.
	460	2126	n–π^* trans.
VO	230	186	π–π^* trans.
	270	324	n–π^* trans.
	290	2086	n–π^* trans.
	365	1220	n–π^* trans.
	435	1893	n–π^* trans.
Y	220	167	n–π^* trans.
	290	245	n–π^* trans.
	360	1680	n–π^* trans.
	390	1440	n–π^* trans.
	430	2138	n–π^* trans.

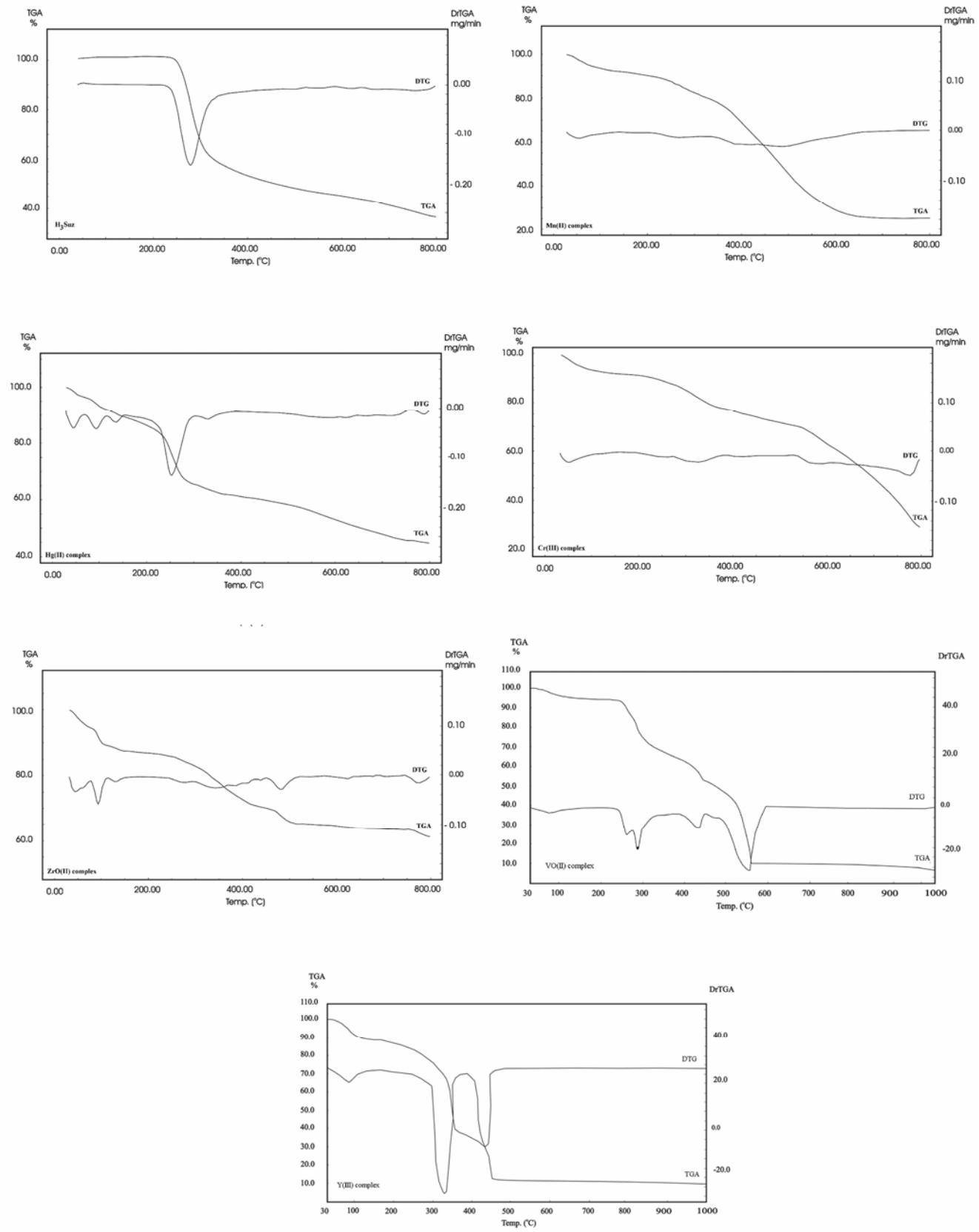

Figure 3. TGA/DTG curves of sulfasalazine and its complexes.

Table 4. Thermal data of sulfasalazine and its complexes.

Compound	Steps	Temp. range (°C)	DTG peak (°C)	TG weight loss (%) Calc.	Found	Assignments
H_3SuZ	1	150–380	279	47·69	47·20	$C_4H_6N_4SO_3$
	2	400–800	752	16·00	16·50	$C_2H_8O_2$
						12C (residue)
$[Mn(SuzH)(H_2O)_4]2H_2O$	1	40–130	54	6·44	6·69	$2H_2O$
($C_{18}H_{24}N_4O_{11}S$ Mn)	2	150–300	271	12·88	12·43	$4H_2O$
	3	340–430	400	13·77	13·82	$C_2H_7NO_2$
	4	440–800	560	39·18	39·60	$C_9H_5N_3SO_2$
						MnO + (7C residue)
$[Hg(SuzH)(H_2O)_2]4H_2O$	1	50–180	94, 137	10·21	10·80	$4H_2O$
($C_{18}H_{24}N_4O_{11}S$ Hg)	2	190–380	254, 333	29·50	29·12	$2H_2O + C_6H_8N_2SO_2$
	3	400–800	780	15·88	16·12	$C_4H_4N_2O_2$
						HgO + (8C residue)
$[Cr(SuzH)(Cl)(H_2O)_3]5H_2O$	1	50–150	60	7·17	7·39	$2{\cdot}5H_2O$
($C_{18}H_{28}N_4O_{13}S$ Cl Cr)	2	170–380	325	15·77	15·69	$5{\cdot}5H_2O$
	3	400–540	490	6·85	6·45	C_2H_5N
	4	560–640	580	6·69	6·56	C_2H_4N
	5	640–800	776	34·18	33·86	$C_5H_3N_2SO_{3.5}Cl$
						$CrO_{1.5}$ + (9C residue)
$[ZrO(SuzH)(H_2O)_2]_8H_2O$	1	10–50	45	5·26	5·67	$2H_2O$
($C_{18}H_{32}N_4O_{15}S$ ZrO)	2	50–90	60	5·26	5·27	$2H_2O$
	3	90–140	100	2·63	2·19	H_2O
	4	140–270	160	5·26	5·73	$2H_2O$
	5	270–450	343	12·29	12·80	$3H_2O + NO$
	6	450–560	482	4·97	4·93	$N_2 + 3H_2$
	7	600–800	775	2·92	2·29	$0{\cdot}5N_2 + 3H_2$
						$ZrOSO_4$ + (18C residue)
$[VO(SuzH)(H_2O)_2]6H_2O$	1	30–110	95	2·96	2·50	H_2O
($C_{18}H_{28}N_4O_{13}S$ VO)	2	110–250	240	4·44	4·29	$1{\cdot}5H_2O$
	3	260–290	280	10·37	10·31	$3{\cdot}5H_2O$
	4	290–350	332	12·85	12·89	$2H_2O + C_2H_2O$
	5	350–400	390	6·91	6·51	C_2H_2O
	6	400–450	440	9·22	9·32	C_2H_2NO
	7	450–550	530	14·49	14·94	C_2H_2NSO
	8	550–800	562	25·04	25·46	$C_{10}H_4N_2$
						VO_2 (residue)
$[Y(SuzH)(Cl)(H_2O)_3]6H_2O$	1	30–95	85	6·59	6·40	$2{\cdot}5H_2O$
($C_{18}H_{30}N_4O_{14}$ S Cl Y)	2	100–190	170	5·27	5·92	$2H_2O$
	3	200–280	260	6·59	6·31	$2{\cdot}5H_2O$
	4	290–320	311	9·08	9·36	$2H_2O + C_2H_2$
	5	320–390	353	23·37	23·85	$C_5H_4N_2SCl$
	6	390–450	435	17·73	18·39	$C_6H_3NO_2$
	7	450–800	470	14·80	15·28	$C_5H_3NO_{1.5}$
						$YO_{1.5}$ (residue)

The complex $[VO(SuzH)(H_2O)_2]6H_2O$ is thermally stable up to 306 K and undergoes decomposition beyond this temperature, as indicated by the first mass loss step in the TG curve. The mass loss at 383 K corresponds to elimination of H_2O molecule (obs = 2·50%, calc = 2·96). Beyond 383 K continuous mass loss in the TG curve has been observed up to 563 K which corresponds to elimination of the remaining H_2O molecules and C_2H_2O (organic moiety) (obs = 27·49%, calc = 27·66). After this decomposition, the mass loss at 563–1073 K corresponds to removal of the rest of sulfasalazine molecule. The DTG profile shows two endothermic and two broad exothermic peaks at 534, 560, 709 and 812 K. The first and the second endothermic peaks appear at 534 and 560 K corresponding to the dehydration of the complex, while the third and fourth exothermic peaks appear at 709 and 812 K corresponding to the decomposition of the organic ligand to the VO_2 (obs = 13·78%, calc = 13·66).

The complex $[Y(SuzH)(Cl)(H_2O)_3]6H_2O$ is thermally stable up to 306 K and undergoes decomposition beyond this temperature, as indicated by the first mass loss step in the TG curve. The mass loss at 368 K corresponds to

Table 5. Kinetic parameters using the Coats–Redfern (CR) and Horowitz–Metzger (HM) operated for the sulfasalazine and its complexes.

Complex	Stage	Method	Parameter					
			E (J mol^{-1})	A (s^{-1})	ΔS (J mol^{-1} K^{-1})	ΔH (J mol^{-1})	ΔG (J mol^{-1})	r
Sulfasalazine	1st	CR	$1{\cdot}31 \times 10^5$	$2{\cdot}13 \times 10^{11}$	$-5{\cdot}23 \times 10$	$1{\cdot}26 \times 10^5$	$1{\cdot}55 \times 10^5$	0·9791
		HM	$1{\cdot}47 \times 10^5$	$9{\cdot}89 \times 10^{10}$	$-2{\cdot}04 \times 10$	$1{\cdot}42 \times 10^5$	$1{\cdot}53 \times 10^5$	0·9993
Mn(II)	3rd	CR	$7{\cdot}85 \times 10^4$	$1{\cdot}45 \times 10^5$	$-1{\cdot}51 \times 10^2$	$7{\cdot}40 \times 10^4$	$1{\cdot}56 \times 10^5$	0·9902
		HM	$8{\cdot}44 \times 10^4$	$1{\cdot}12 \times 10^6$	$-1{\cdot}34 \times 10^2$	$7{\cdot}99 \times 10^4$	$1{\cdot}53 \times 10^5$	0·9961
Hg(II)	2nd	CR	$1{\cdot}25 \times 10^5$	$2{\cdot}57 \times 10^{10}$	$-5{\cdot}04 \times 10$	$1{\cdot}40 \times 10^5$	$1{\cdot}48 \times 10^5$	0·9997
		HM	$1{\cdot}34 \times 10^5$	$2{\cdot}76 \times 10^{11}$	$-3{\cdot}06 \times 10$	$1{\cdot}30 \times 10^5$	$1{\cdot}46 \times 10^5$	0·9985
Cr(III)	2nd	CR	$9{\cdot}37 \times 10^5$	$3{\cdot}57 \times 10^5$	$-1{\cdot}44 \times 10^2$	$8{\cdot}87 \times 10^4$	$1{\cdot}75 \times 10^5$	0·9960
		HM	$6{\cdot}09 \times 10^5$	$2{\cdot}98 \times 10^6$	$-1{\cdot}08 \times 10^2$	$1{\cdot}04 \times 10^5$	$1{\cdot}68 \times 10^5$	0·9999
ZrO(II)	3rd	CR	$1{\cdot}02 \times 10^5$	$1{\cdot}98 \times 10^6$	$-1{\cdot}30 \times 10^2$	$9{\cdot}71 \times 10^4$	$1{\cdot}78 \times 10^5$	0·9944
		HM	$1{\cdot}14 \times 10^5$	$4{\cdot}21 \times 10^7$	$-1{\cdot}05 \times 10^2$	$1{\cdot}09 \times 10^5$	$1{\cdot}74 \times 10^5$	0·9985
VO(II)	1st	CR	$3{\cdot}41 \times 10^4$	$5{\cdot}43 \times 10^2$	$-1{\cdot}94 \times 10^2$	$3{\cdot}11 \times 10^4$	$1{\cdot}02 \times 10^5$	0·9917
		HM	$4{\cdot}10 \times 10^4$	$7{\cdot}34 \times 10^3$	$-1{\cdot}73 \times 10^2$	$3{\cdot}80 \times 10^4$	$1{\cdot}01 \times 10^5$	0·9990
Y(III)	1st	CR	$5{\cdot}45 \times 10^4$	$8{\cdot}67 \times 10^5$	$-1{\cdot}33 \times 10^2$	$5{\cdot}15 \times 10^4$	$9{\cdot}91 \times 10^4$	0·9996
		HM	$6{\cdot}14 \times 10^4$	$1{\cdot}29 \times 10^7$	$-1{\cdot}10 \times 10^2$	$5{\cdot}84 \times 10^4$	$9{\cdot}79 \times 10^4$	0·9998

Table 6. Antimicrobial activity of sulfasalazine and its complexes.

Tested compounds	Diameter of inhibition zone (cm)			
	B. subtilis	*E. coli*	*P. rotatum*	*T. sp.*
H_3Suz	0	1	0	0
Mn(II)	0	1	0	1
Hg(II)	0	0	0	2
Cr(III)	0	0	0	0·6
ZrO(II)	0	0	0	0
VO(II)	0	0	0	0
Y(III)	0	0	0	0
Control	0	0	0	0

elimination of 2·5H_2O molecules (obs = 6·40%, calc = 6·59). Beyond 368 K continuous mass loss in the TG curve has been observed up to 563 K which corresponds to removal of the remaining H_2O molecules and C_2H_2 (organic moiety) (obs = 21·59%, calc = 20·94). After this decomposition, the mass loss at 593–1073 K corresponds to decomposition of the rest of sulfasalazine molecule. The DTG profile shows two exothermic peaks at 616 and 716 K. The first exothermic peak appears at 616 K corresponding to the elimination of $C_5H_4N_2SCl$ (organic moiety) (obs = 23·85%, calc = 23·37), while the second peak appears at 716 K corresponding to the decomposition of the organic ligand to the $YO_{1.5}$ (obs = 16·57%, calc = 16·54).

In the present investigation, the general thermal behaviours of the sulfasalazine complexes in terms of stability ranges, peak temperatures and values of kinetic parameters, are shown in table 4. The kinetic and thermodynamic parameters have been evaluated using the Coats–Redfern and Horowitz–Metzger equations (Horowitz and Metzger 1963; Coats and Redfern 1964; Osowole *et al* 2002).

The entropy of activation, ΔS^*, was calculated. The enthalpy activation, ΔH^*, and Gibbs free energy, ΔG^*, were calculated from $\Delta H^* = E^* - RT$ and $\Delta G^* = \Delta H^* - T\Delta S^*$, respectively. The thermodynamic behaviour of all complexes of sulfasalazine with transition metal ions is non-spontaneous (more ordered) reactions (ΔS is negative value), endothermic reactions ($\Delta H > 0$) and endergonic ($\Delta G > 0$), during the reactions.

The thermodynamic data obtained with the two methods are in harmony with each other. The activation energy of Cr^{+3} and Hg^{+2} complexes is expected to increase in relation with decrease in their radii (Abd El-Wahed *et al* 2008a–d). The smaller size of the ions permits a closer approach of the ligand. Hence, the E value in the second stage for the Cr^{+3} complex is higher than that for the other Hg^{+2} complex. The correlation coefficients of the Arrhenius plots of the thermal decomposition steps were found to lie in the range 0·9791–0·9999, showing a good fit with linear function. It is clear that the thermal decomposition process of all H_3Suz complexes is non-spontaneous, i.e. the complexes are thermally stable.

The thermograms and the calculated thermal parameters for the complexes show that the stability of these complexes depends on the nature of the central metal ion. It can be seen from the curves that the thermal stability of ZrO(II) complex is higher than that for the corresponding VO(II) complex with the same ligand. The decomposition temperature of ZrO(II) complex lies at 775°C, but the VO(II) complex decomposes to the oxide at 562°C. The thermal stability of the metal complexes was found to increase periodically with increase in atomic number of the metal and the larger value of charge/radius ratio (Malik *et al* 1984).

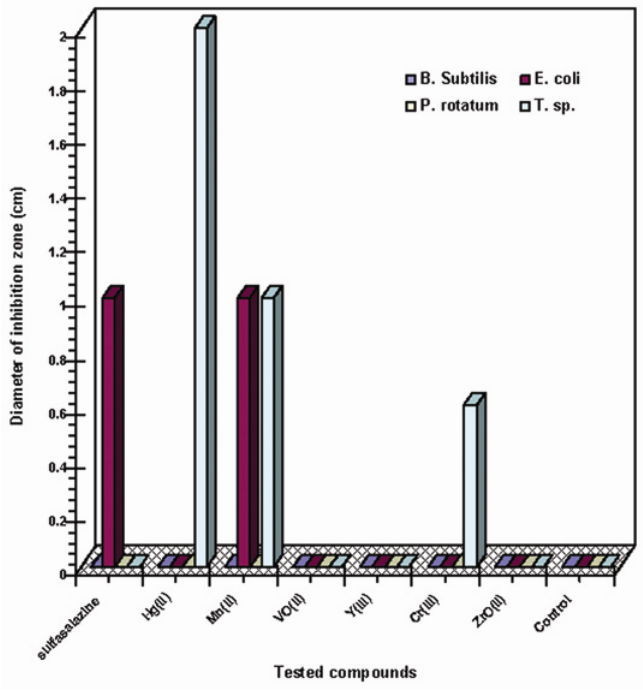

Figure 4. Microbial test for sulfasalazine and its complexes.

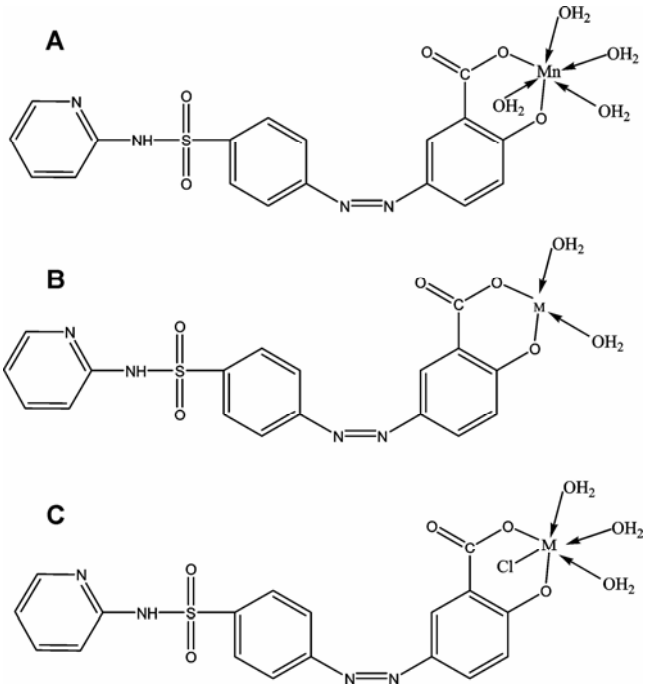

Figure 5. **A**. Structure of Mn(II)/HSuz complex, **B**. structure of M(II)/HSuz complex (where M = Hg(II), ZrO(II) and VO(II)) and **C**. structure of M(III)/HSuz complex (where M = Cr(III) and Y(III)).

3.5 *Antimicrobial activity*

Antibacterial and antifungal activities of the ligand and its complexes were carried out against *Escherichia coli* (Gram, –ve), *Bacillus subtilis* (Gram, +ve) and antifungal (tricoderma and penicillium activities). The results of the antimicrobial test are given in table 6 and shown in figure 4. The antimicrobial activity was estimated on the basis of size of inhibition zone around dishes. The ligand and complexes were less active against *Bacillus subtilis* and penicillium, whereas Hg(II)/HSuz is more active rather than Cr(III) and Mn(II) complexes against tricoderma.

References

Abdel-Gawad F M, el-Guindi N M and Ibrahim M N 1987 *J. Drug Res.* **17** 197

Abd El-Wahed M G, Refat M S and El-Megharbel S M 2008a *Spectrochim Acta* **A70** 916

Abd El-Wahed M G, Refat M S and El-Megharbel S M 2008b *J. Mol. Struct.* (in press)

Abd El-Wahed M G, Refat M S and El-Megharbel S M 2008c *J. Mol. Struct.* (in press)

Abd El-Wahed M G, Refat M S and El-Megharbel S M 2008d *Mens Agitat.* **3** (in press)

Anacona J R 2001 *J. Coord. Chem.* **54** 355

Bell C M and Habal F M 1997 *Am. J. Gastroenterol.* **92** 2201

Brown D H, Lewis A E, Smith W E and Teape J W 1980 *J. Med. Chem.* **23** 729

Chen Z -F, Kang S, Liang H, Yi F, Yu K -B, Xiong R -G and You X -Z 2003 *Appl. Organometal. Chem.* **17** 887

Chen Z -F, Kang S, Shi S -M, Abrahams B F and Liang H 2008 *J. Mol. Struct.* **882** 134

Coats A W and Redfern J P 1964 *Nature* **201** 68

Deacon G B and Phillips R J 1980 *Coord. Chem. Rev.* **33** 227

Diav-Citrin O *et al* 1998 *Gastroenterology* **114** 23

Geary W J 1971 *Coord. Chem. Rev.* **7** 81

Golzar Hossain G M, Amoroso A J, Banu A and Malik K M A 2007 *Polyhedron* **26** 967

Gupta R, Saxena R K, Chatarvedi P and Virdi J S 1995 *J. Appl. Bacteriol.* **78** 378

Hanauer S B *et al* 2005 *Am. J. Gastroenterol.* **100** 2478

Helaleh M I H and Nameh E S M 1998 *An. Quim. Int. Ed.* **94** 160

Horowitz H W and Metzger G 1963 *Anal. Chem.* **35** 1464

Kang S, Chen Z -F and Guangxi J 2006 *Normal University* **26** 789

Klostersky J, Danean D and Weerts D 1973 *Chemotherapy* **18** 191
Lever A B P 1980 *Inorganic electronic spectroscopy* (London: Elsevier) 4th ed, p. 481
Lozano J and Borras J 1987 *J. Inorg. BioChem.* **31** 187
Malik W, Tuli G D and Madan R D 1984 *Selected topics in inorganic chemistry* (New Delhi: Chand and Co. Ltd.)
Mukherjee G N, Basu S and Ghosh T 1993 *J. Indian Chem. Soc*. **70** 1043
Nakamoto K 1986 *Infrared and Raman spectra of inorganic and coordination compounds* (New York: Wiley) 4th ed
Osowole A A, Woods J A O, Fagade O E and Odunola O A 2002 *Biosci. Res. Commun*. **14** 531
Refat M S 2007 *J. Mol. Struct*. **842** 24
Ruiz M, Perello L, Ortiz R, Castineiras A, Maichlemossmer C and Canton E 1995 *J. Inorg. Biochem*. **59** 801
Sorenson J R J 1976 *J. Med. Chem*. **19** 135
Sutherland L *et al* 2000 *Cochrane Database Syst. Rev*. CD000543
Tabassum S, Arimand F and Rafiqi S H 1996 *Main Group Metal Chem*. **19** 245
Wang X -S, Song Y -M and Xiong R -G 2005 *Chin. J. Inorg. Chem*. **21** 1277
Williams D R 1971 *The metals of life* (London: Van Nostrand Reinhold)
Yuan R -X, Shi J -D and Yang G -W 2006 *Chin. J. Inorg. Chem*. **22** 877
Zaki A, Schreiber E C, Weliky I, Knill J R and Hubsher H J 1974 *J. Clin. Pharmacol*. **14** 1180